A Multi-Atlas and Label Fusion Approach for Patient-Specific MRI Based Skull Segmentation

Angel Torrado-Carvajal[1,2], Juan A. Hernandez-Tamames[1,2], Joaquin L. Herraiz[2], Yigitcan Eryaman[2,3], Yves Rozenholc[4], Elfar Adalsteinsson[5,6], Lawrence L. Wald[3,6], and Norberto Malpica[1,2]

[1]Dept. of Electronics, Universidad Rey Juan Carlos, Mostoles, Madrid, Spain, [2]Madrid-MIT M+Vision Consortium in RLE, MIT, Cambridge, Massachusetts, United States, [3]Dept. of Radiology, MGH, Martinos Center for Biomedical Imaging, Charlestown, Massachusetts, United States, [4]MAP5, CNRS UMR 8145, University Paris Descartes, Paris, Paris, France, [5]Dept. of Electrical Engineering and Computer Science, MIT, Cambridge, Massachusetts, United States, [6]Harvard-MIT Health Sciences and Technology, MIT, Cambridge, Massachusetts, United States

Target Audience: MRI researchers and clinicians who are interested in patient-specific bone segmentation methods based only on MRI.

Purpose: Bone segmentation is an important task that should be performed for accurate construction of patient-specific models. [1] The electromagnetic and physical properties of the skull are different from soft tissue; therefore the bone segmentation should be handled separately for model construction. Most approaches to patient-specific model creation combine MR images with CT images [2,3], leveraging the benefits of differentiating soft tissues and bone respectively. However, CT images require the use of radiation and additional costs and time, while segmentation of the skull based only on MRI is a challenging problem due to the lack of signal in bone tissues as well as in air. Thus, we propose a method for complete skull segmentation based only on T1-weighted images of the human head.

Methods: ***Data Acquisition:*** Images of the head were acquired on a General Electric Signa HDxt 3.0T MR scanner using the body coil for excitation and an 8-channel quadrature brain coil for reception. Imaging was performed using an isotropic 3DT1w SPGR sequence with a TR=10.024ms, TE=4.56ms, TI=600ms, NEX=1, acquisition matrix=288x288, resolution=1x1x1mm, flip angle=12.

Data Preprocessing: Image preprocessing was carried out using 3D Slicer built-in modules [4]. The preprocessing steps included: MRI bias correction (N4 ITK MRI bias correction), and registration (BRAINS) for movement correction.

Segmentation: The skull is estimated using a multi-atlas segmentation and label-fusion approach. We consider the CT volumes from the whole head CT-scan database [5]. These CTs are registered to the patient MRI image using affine and non-rigid transformations. These registration steps are performed with the NiftyReg Aladin [6,7] and Fast Free-Form Deformation [8,9] algorithms using the Normalised Mutual Information gradient. Each CT volume is then automatically segmented to obtain the skull. Thresholding is performed in this step instead of registering the original segmentations so as to minimize computational time. The final patient-specific skull is estimated using label fusion techniques; we have compared Majority Voting, the Simultaneous Truth and Performance Level Estimation (STAPLE) [10], and the Selective and Iterative Method for Performance Level Estimation (SIMPLE) [11] algorithms.

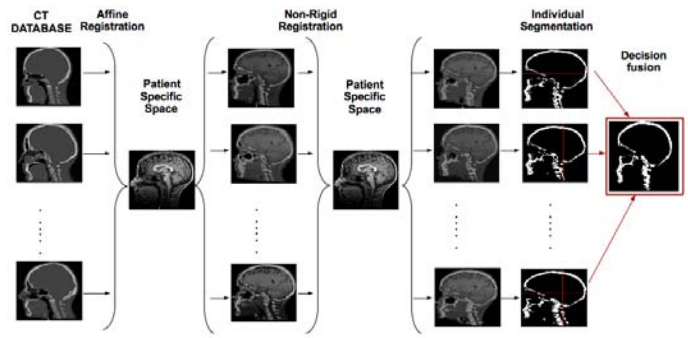

Fig. 1. Skull Segmentation Estimation Pipeline based only on Patient-Specific MRI. The different CT images of the multi-atlas are registered (affine and non-rigid) to the unseen MRI data space. Then, threshold segmentation of the CTs is performed and label fusion is applied, obtaining the patient-specific skull.

Results: The method was fully automated and spent about 1 hour running over Ubuntu Precise (12.04.3 LTS) on an Intel(R) Core(TM) i7-2600 CPU @ 3.40GHz with 8GB RAM. The method was tested in 12 healthy subjects (4 males/ 8 females) aged 22-57 participating in this study. The CT database included 19 healthy subjects (9 males/10 females) aged 25-42 from the [5] previous study. Figure 2 shows the skull estimation over several slices of a single subject, where we can appreciate the differentiation between bone and air. The comparison between the label fusion techniques provided Dice similarity indexes over 0.96 and Haussdorf distances below 4.3mm. Visual inspection evaluation of the estimated segmentation was performed by an expert radiologist, considering all the segmentations as accurate. Figure 3 shows the reconstruction of the skull for 10 subjects in the study.

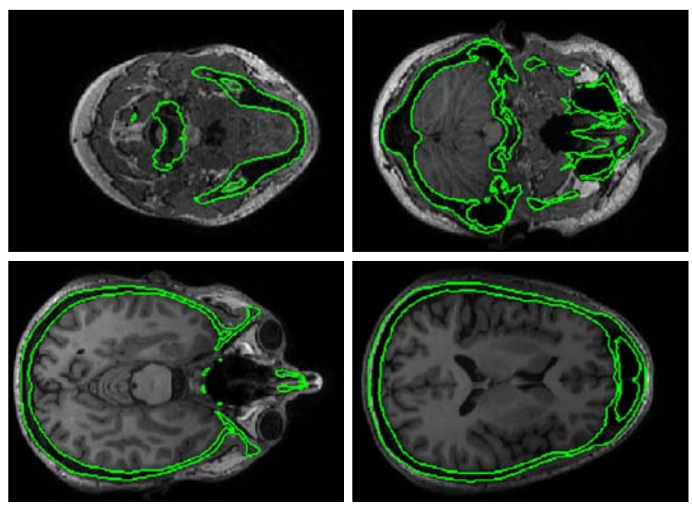

Fig. 2. Skull estimation on several slices of the whole head of a single subject. The contour shows how the approach differentiates between bone and air.

Discussion: The segmentation of the skull based on patient-specific only MRI is feasible with a previous CT multi-atlas approach and label-fusion techniques. The results are promising and may allow removing patient-specific CT acquisitions in several protocols such as brain studies with PET-MRI scanners [12]. This approach provides good results, but computing many non-rigid registrations is expensive. However, the pipeline can be accelerated by including a selection of similar atlases step after the affine registration. Real accuracy of the approach may be evaluated by acquiring CT-MRI pairs of several subjects.

Conclusion: We present a new multi-atlas and label-fusion segmentation approach to segment the skull based only on patient-specific MRI. The estimation of the skull adjusts to the bone boundary limits while differentiates the air. The use of this approach may lead to a decrease in patient ionization by removing patient-specific CT acquisitions.

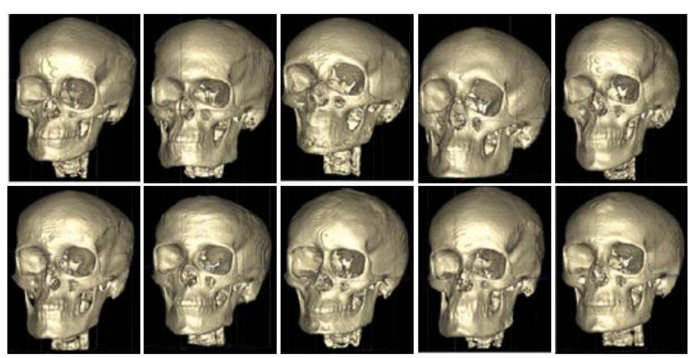

Fig. 3. Reconstruction of the skull estimation for ten subjects in the study. In this representation we can appreciate the level of detail of the approach.

References

[1] Wolf, S., et al. Magnet Reson Med 2013, Apr;69(4):1157–68.
[2] Homann, H., et al. Magnet Reson Med 2011, Dec;66(6):1767–76.
[3] Jin, J., Phys Med Biol 2012, Dec;57(24):8153–712.
[4] Pieper, S., et al. ISBI 2004, Apr;1:632–635.
[5] Tilotta, F., et al. Forensic Sci Int 2009, Oct;191(1):112–e1.
[6] Ourselin, S., et al. Image Vision Comput 2001, Jan;19(1-2):25–31.
[7] Ourselin S., et al. MICCAI 2002, 140–47.
[8] Modat M., et al. Comput Meth Prog Bio 2009, Jun;98(3):278–84.
[9] Rueckert, D., et al. IEEE Trans Med Imag 1999, Aug;18(8):712–721.
[10] Warfield, S., et al. IEEE T Med Imaging 2004, Jul;23(7):903–21.
[11] Langerak, T.R., et al. IEEE T Med Imaging 2010, Dec;29(12):2000–8.
[12] Andersen F.L., et al. Neuroimage 2013, Aug;84:206–16.

Acknowledgements: This project is supported by the Comunidad de Madrid and the Madrid MIT M+Vision Consortium.